JOURNAL OF
Materials
CHEMISTRY

Crystal structures, and electrical conduction and magnetic properties in $CuCl_4$ salts of dimethylthio- and ethylenedithio-tetrathiafulvalenothioquinone-1,3-dithiolemethides

Masaki Iwamatsu,[a] Tsuyoshi Kominami,[a] Kazumasa Ueda,[a] Toyonari Sugimoto,*[a] Toshiji Tada,[a] Kei-ichiro Nishimura,[a] Tomohiro Adachi,[b] Hideo Fujita,[c] Fangzhun Guo,[d] Shoichi Yokogawa,[d] Harukazu Yoshino,[d] Keizo Murata[d] and Motoo Shiro[e]

[a]*Research Institute for Advanced Science and Technology, Osaka Prefecture University, Sakai, Osaka 599-8570, Japan. E-mail: toyonari@iwate.riast.osakafu-u.ac.jp*
[b]*Department of Chemistry, Faculty of Integrated Arts and Sciences, Osaka Prefecture University, Sakai, Osaka 599-8531, Japan*
[c]*Department of Natural Environment, Faculty of Integrated Human Studies, Kyoto University, Kyoto 606-8501, Japan*
[d]*Graduate School of Science, Osaka City University, Sumiyoshi, Osaka 558-8585, Japan*
[e]*Rigaku Corporation, Akishima, Tokyo 196-8666, Japan*

Received 31st July 2000, Accepted 25th October 2000

The reaction of dimethylthio- (**1**) and ethylenedithio-tetrathiafulvalenothioquinone-1,3-dithiolemethides (**2**) with $CuCl_2$ afforded the corresponding $CuCl_4$ salts, $(\mathbf{1})_2\cdot CuCl_4$ and $(\mathbf{2})_3\cdot CuCl_4$. For $(\mathbf{1})_2\cdot CuCl_4$ the **1** molecules are stacked to form a one-dimensional column, and in each column the neighboring **1** molecules are dimerized. On the other hand, the **2** molecules in $(\mathbf{2})_3\cdot CuCl_4$ are stacked one-dimensionally in a triad unit. The $CuCl_4$ ions intervene between the **1**- or **2**-stacked columns in each case. The electrical resistivities (ρ) for single crystals of $(\mathbf{1})_2\cdot CuCl_4$ and $(\mathbf{2})_3\cdot CuCl_4$ were 3×10^4 and $0.6\ \Omega$ cm at room temperature, respectively. The ρ value of $(\mathbf{2})_3\cdot CuCl_4$ increased continuously on cooling, and its activation energy was 0.15 eV, which became gradually smaller with increasing applied pressure. For $(\mathbf{1})_2\cdot CuCl_4$ the Cu(II) spins on the $CuCl_4$ ions were only present whilst $(\mathbf{2})_3\cdot CuCl_4$ involved both conducting π electrons on the **2**-stacked column and localized Cu(II) spins on the $CuCl_4$ ions which did not interact with each other between 300 and *ca.* 170 K, but below *ca.* 170 K the conducting π electrons disappeared, presumably as a result of interaction with the localized d spins.

Introduction

The synthesis of organic solids involving both conducting π electrons and localized d spins is of current interest, since novel electrical conduction and magnetic properties might be produced, if both components can undergo significant interaction with one another.[1] Several π/d-cooperative molecular systems are so far known, but are limited to copper-[2] and cobalt-phthalocyanines,[3] copper dimethyldicyanoquinodiimine (DMe-DCNQI),[4] and bis(ethylenedithio)-tetrathiafulvalene (BEDT-TTF) and -tetraselenafulvalene (BEDT-TSF) radical cation salts with copper or iron counter-anions.[5–8] Furthermore, the degree of π/d interaction is very weak for almost all the molecular systems, except for $(\text{DMe-DCNQI})_2\cdot Cu$,[9] $(\text{BEDT-TTF})_3\cdot CuBr_4$,[10] $(\text{BEDT-TTF})_3\cdot CuCl_2Br_2$,[10] λ-$(\text{BEDT-TSF})_2\cdot FeCl_4$,[11] and κ-$(\text{BEDT-TSF})_2\cdot FeBr_4$,[12] which exhibit significant π/d interaction and novel electrical conduction/magnetic properties. In order to understand more fully the π/d interaction and also to create unprecedented molecular-based organic metal magnets, much attention is being directed towards new π/d-cooperative molecular systems, especially those based on new donor molecules. Very recently, we have succeeded in synthesising a new donor molecule, **1**, which still maintains an electron-donating ability comparable to TTF and can also interact with several magnetic-metal salts effectively *via* coordination to the thiocarbonyl sulfur atom.[13] In this paper we report on the synthesis of another new donor molecule, **2**, and the crystal structures and electrical conduction/magnetic properties in $CuCl_4$ salts of **1** and **2**, $(\mathbf{1})_2\cdot CuCl_4$ and $(\mathbf{2})_3\cdot CuCl_4$, and furthermore discuss the possibility of π/d interaction in these $CuCl_4$ salts.

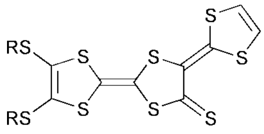

1: R = CH_3
2: R, R = $-CH_2CH_2-$

Experimental

Synthesis of 2, $(\mathbf{1})_2\cdot CuCl_4$ and $(\mathbf{2})_3\cdot CuCl_4$

By a similar procedure to the synthesis of **1**,[13] **2** was successfully obtained. Thus, the zinc complex of bis(tetraethylammonium) bis(2,3-ethylenedithiotetrathiafulvalenyl-6,7-dithiolato)[14] (400 mg, 0.37 mmol) was reacted with 2 equiv. of 2-methylthio-1,3-dithiolium tetrafluoroborate[15,16] (194 mg, 0.82 mmol) in THF–DMF (1 : 1 (v/v)) containing 1% (v/v) acetic acid at −70 °C under argon. After separation of the reaction mixture by column chromatography on silica gel (solvent: CS_2), followed by recrystallization from CS_2–MeOH, **2** was isolated as black crystals (mp 186–187 °C) in 45% yield. ^1H NMR ($CDCl_3$, 300 MHz): δ 7.46 (1H, d, $J = 6.30$ Hz), 7.30 (1H, d, $J = 6.30$ Hz), 2.41 (4H, s). Anal. Calcd. for $C_{11}H_6S_9$: C, 30.96; H, 1.42. Found: C, 31.01; H, 1.63%.

DOI: 10.1039/b006173p

When **1** (8.6 mg, 0.02 mmol) in CS_2 (3 ml) was mixed with $CuCl_2$ (27 mg, 0.2 mmol) in CH_3CN (3 ml) at room temperature for 1 week, (**1**)$_2$·$CuCl_4$ was isolated as black plates (mp > 300 °C) in 91% yield. Anal. Calcd. for $C_{22}H_{16}S_{18}Cl_4Cu$ (1062.9): C, 24.86; H, 1.52. Found: C, 24.75; H, 1.73%. By a similar procedure [(**2**)$_3$·$CuCl_4$]·$(CS_2)_2$ was isolated as black plates (mp > 300 °C) in 85% yield. Calcd. for $C_{35}H_{18}S_{31}Cl_4Cu$ (1638.0): C, 25.67; H, 1.11. Found: C, 25.72; H, 1.28%.

X-Ray data collection, structure solution and refinement

Intensity data of **2**, (**1**)$_2$·$CuCl_4$ and (**2**)$_3$·$CuCl_4$ at 293 K were collected on a Rigaku AFC5R diffractometer using Mo-Kα radiation ($\lambda = 0.71069$ Å). Intensity data of (**2**)$_3$·$CuCl_4$ at 200 and 120 K were collected on a Rigaku RAXIS-IV imaging plate diffractometer with graphite monochromated Mo-Kα radiation ($\lambda = 0.71069$ Å). In the solution and refinement of these structures, the teXsan crystallographic software package was used.[17] Data were corrected for absorption by empirical methods. The structures were solved by direct methods, and refined on F_o^2 with full-matrix least-squares analysis. The hydrogen atoms were placed at calculated positions and refined according to a riding model. Crystal data and details of the data collection on **2**, (**1**)$_2$·$CuCl_4$ and [(**2**)$_3$·$CuCl_4$]·$(CS_2)_2$ are summarized in Table 1. For [(**2**)$_3$·$CuCl_4$]·$(CS_2)_2$ the crystal structure determinations were performed at 293, 200 and 120 K. In an asymmetric unit, one ordered and one half-disordered molecule of **2** is present together with a half of one $CuCl_4$ anion and one disordered CS_2 molecule. The skeletal ring of the disordered molecule was refined as an averaged structure with unit occupancy. CCDC reference number 1145/261. See http://www.rsc.org/suppdata/jm/b0/b006173p/ for crystallographic files in .cif format.

Electrical resistivity, magnetic susceptibility and ESR measurements

The ρ values were measured on single crystals of (**1**)$_2$·$CuCl_4$ using a voltage-driven two-probe method at room temperature and of (**2**)$_3$·$CuCl_4$ using a four-probe method in the temperature range 120 to 300 K. The contact to the electrode was achieved with a gold paste. The magnetic measurement of the $CuCl_4$ salts was performed in the temperature range 5 to 300 K under an applied magnetic field of 1 kOe using a SQUID magnetometer (MPMS XL, Quantum Design). The paramagnetic susceptibility (χ_p) was obtained by subtracting the diamagnetic contribution, calculated by a Pascal method, from the observed magnetic susceptibility. ESR spectra of the $CuCl_4$ salts were recorded using a JEOL 1X spectrometer. For determination of the g value a sample of $MnSO_4 \cdot H_2O$ diluted with MgO was used as a reference.

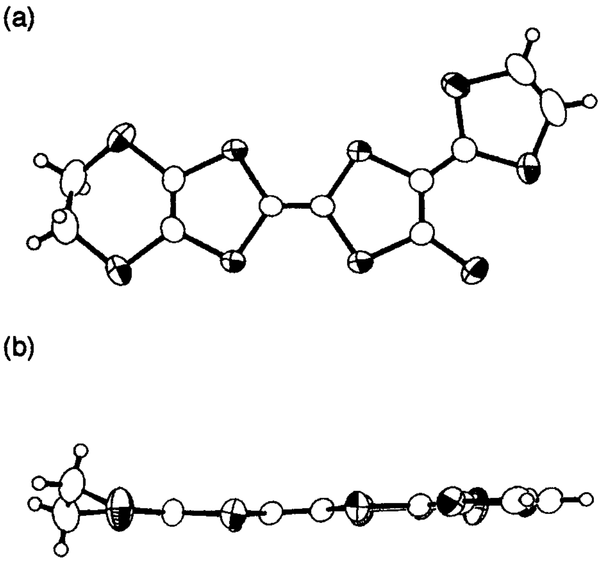

Fig. 1 Molecular structure of **2**: (a) top and (b) side views.

Results and discussion

Molecular structure and redox properties of 2

Fig. 1 shows the molecular structure of **2**. The overall molecular skeleton, including an ethylenedithio group, is almost planar. The thiocarbonyl bond distance is 1.66 Å, which is the same as that of **1**[13] and close to those of normal α,β-unsaturated thioketones.[18] The first and second redox potentials of **2** are +0.60 and +0.80 V *vs.* Ag/AgCl, which are almost the same as those of **1** (+0.61 and +0.77 V).[13] Since these values for **1** and **2** are only higher by 0.1–0.2 V than those of BEDT–TTF (+0.50 and +0.63 V), **2** is also expected to maintain a high electron-donating ability comparable to that of **1**.

Crystal structures of (1)$_2$·CuCl$_4$ and (2)$_3$·CuCl$_4$

The stacking structure of (**1**)$_2$·$CuCl_4$ is shown in Fig. 2a, together with the contacts between the neighboring molecules of **1**. The skeleton of each molecule of **1** is almost planar except for one methylthio group. The **1** molecules are alternately stacked in a reverse direction to form a one-dimensional column along the b axis. Furthermore, in each column the **1**

Table 1 Crystallographic data for **2** and (**1**)$_2$·$CuCl_4$ at 293 K, and [(**2**)$_3$·$CuCl_4$]·$(CS_2)_2$ at 293, 200 and 120 K

	2	(**1**)$_2$·$CuCl_4$	[(**2**)$_3$·$CuCl_4$]·$(CS_2)_2$		
Empirical formula	$C_{11}H_6S_9$	$C_{11}H_8S_9Cl_4Cu$	$(C_{11}H_6S_9)_3 \cdot Cl_4Cu \cdot 2CS_2$		
Formula weight, M	426.7	531.40	1637.8		
Crystal system	Monoclinic	Triclinic	Monoclinic		
Space group	$P2_1/c$	$P\bar{1}$	$C2/c$		
μ/cm^{-1}	12.34	19.09	16.56	16.97	17.04
$R1$,[a] $wR2$[b]	0.042, 0.080	0.071, 0.132	0.094, 0.231	0.064, 0.170	0.074, 0.190
a/Å	7.877(4)	9.517(4)	33.851(4)	33.738(1)	33.708(2)
b/Å	14.141(2)	14.076(6)	10.79(1)	10.6239(3)	10.5740(4)
c/Å	14.541(2)	7.789(2)	16.474(3)	16.3825(6)	16.4010(8)
α/°		94.11(3)			
β/°	100.35(2)	109.37(3)	95.38(1)	95.522(1)	95.609(2)
γ/°		70.69(3)			
V/Å^3	1593.4(8)	928.2(7)	5988(7)	5844.4(4)	5817.9(4)
T/K	293	293	293	200	120
Z	4	2	4	4	4
No. of unique reflections	3653	5346	8706	4533	4598
No. of reflections used	1956	2096	2486	3004	3311

[a] $R1 = (\Sigma||F_o| - |F_c||)/(\Sigma|F_o|)$. [b] $wR2 = [\Sigma w(F_o^2 - F_c^2)^2/\Sigma w(F_o^2)^2]^{1/2}$.

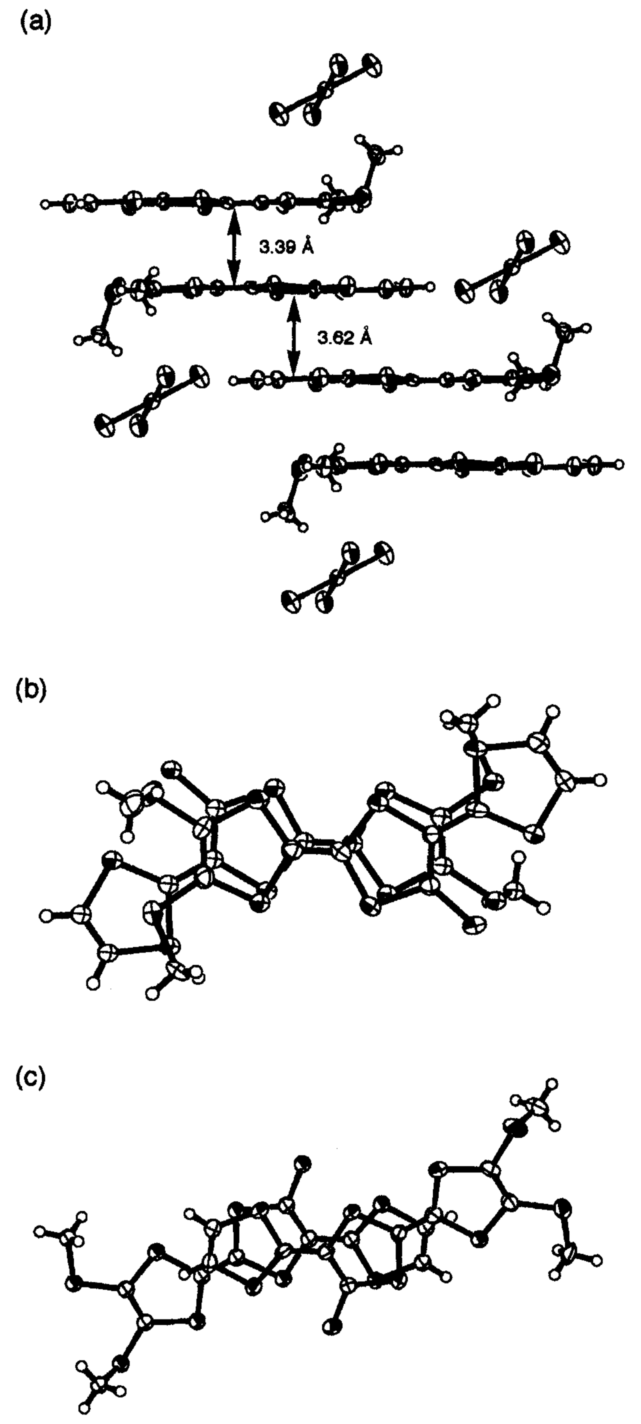

Fig. 2 Crystal structure of $(\mathbf{1})_2\cdot\mathrm{CuCl}_4$ at 293 K: (a) stacking structure, and (b) intradimer and (c) interdimer contacts between the neighboring **1** molecules.

molecules are preferentially dimerized, as shown from the shorter interplanar distance (3.39 Å) than that for a plane of aromatic hydrocarbon rings ("a π-cloud thickness," of 3.50 Å)[19] and also from the effective overlap between the dihydrotetrathiafulvalene rings (Fig. 2b). The interplanar distance between the neighboring dimers is 3.62 Å and the overlap is not so effective (Fig. 2c). The CuCl_4 anion has a complete square-planar geometry, since the four Cu–Cl bond distances are all equal (2.27 Å), the four chlorine atoms are on the same plane and the angles (89.6 and 90.4°) between the neighboring chlorine atoms are close to 90°. There are several contacts between **1** and the CuCl_4 anion, and the distances are 3.20–3.54 Å, which are shorter than the sum (3.65 Å) of the van der Waals' radii of the sulfur and chlorine atoms.

On the other hand, the crystal structure of $(\mathbf{2})_3\cdot\mathrm{CuCl}_4$ measured at 293 K was of poor quality as a result of the large thermal motion of all the atoms. However, when the measurement temperature was lowered to 200 K, the analysis was made with a satisfactory refinement, suggesting that the thermal motion was suppressed as much as possible. The projections down to the *c* and *b* axes, and to the [201] plane are shown in Fig. 3a–c. In the crystal, two crystallographically-independent molecules, **A**(**A**′) and **B** are present. As discussed later, the CuCl_4 anion is actually in the state of CuCl_4^{2-}, so that a unit of three **A**, **A**′ and **B** molecules must possess two positive charges in order to maintain the electrical neutrality of a formula unit of $(\mathbf{2})_3\cdot\mathrm{CuCl}_4$. Since there is almost no difference in the bond distances between molecules **A**(**A**′) and **B**, it is supposed that each molecule has a charge of +(2/3). However, the accurate charge distribution must be estimated by Raman

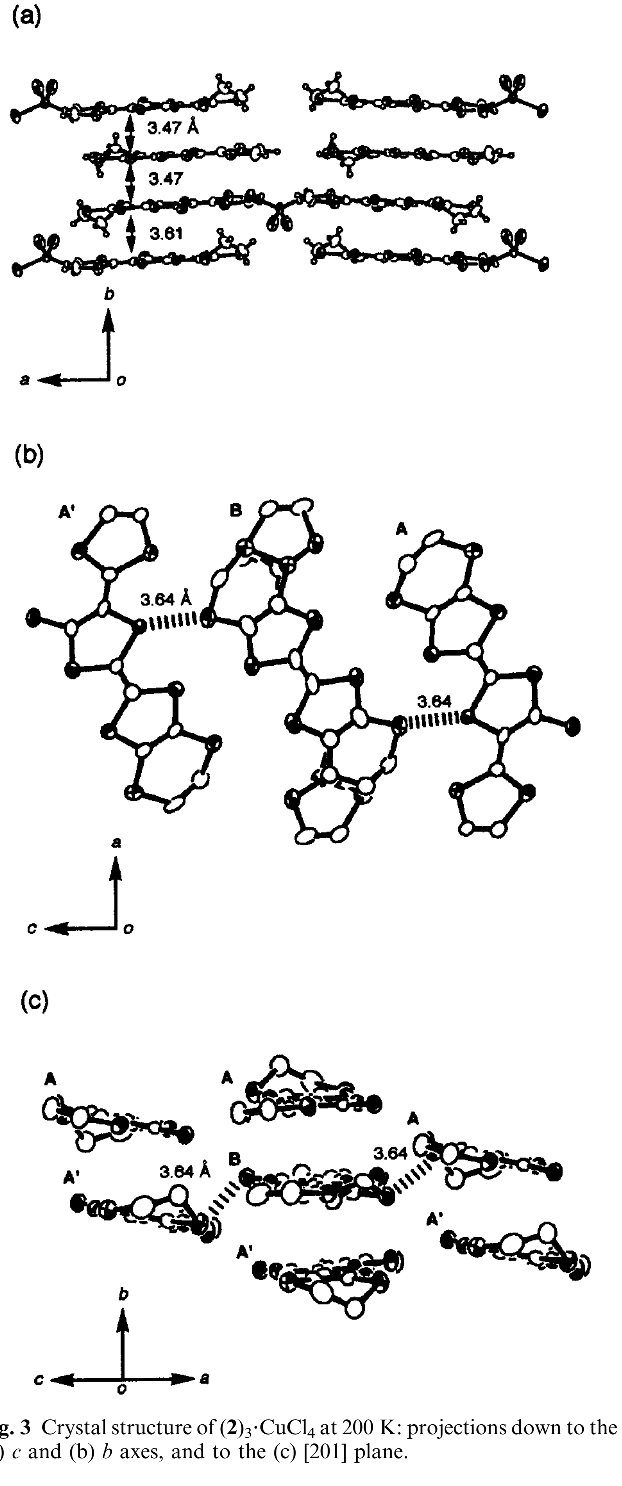

Fig. 3 Crystal structure of $(\mathbf{2})_3\cdot\mathrm{CuCl}_4$ at 200 K: projections down to the (a) *c* and (b) *b* axes, and to the (c) [201] plane.

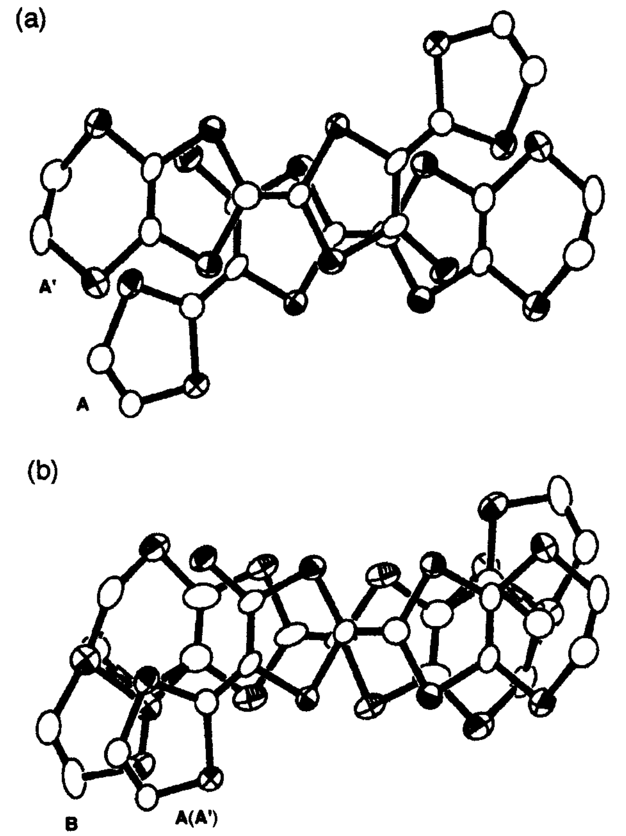

Fig. 4 Contacts (a) between **A** and **A**′, and (b) between **A**(**A**′) and **B** in $(\mathbf{2})_3\cdot\mathrm{CuCl_4}$.

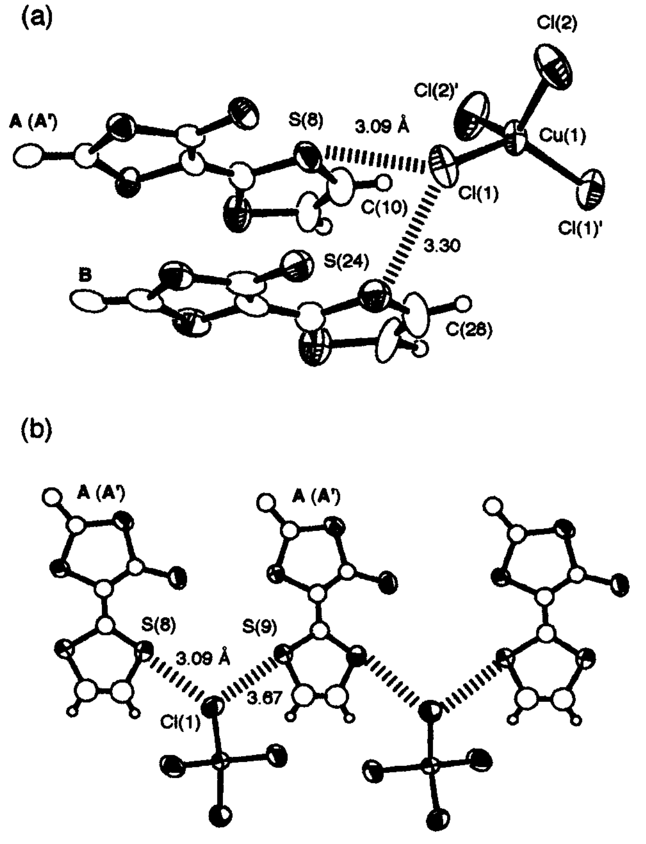

Fig. 5 Contacts of **A**(**A**′)/$\mathrm{CuCl_4}$ and **B**/$\mathrm{CuCl_4}$ in $(\mathbf{2})_3\cdot\mathrm{CuCl_4}$: (a) side and (b) top views. The interatomic distances due to the crystal structure determination at 200 K are shown.

and other spectroscopies. The units composed of the **A** and **A**′ molecules pointing in opposite directions and of the intervening **B** molecule, are repeatedly stacked along the *b* axis to form a one-dimensional column. As seen from Fig. 3a and also Fig. 4, showing **A**/**A**′ and **A**(**A**′)/**B** contacts, the **A** and **A**′ molecules are separated by a much larger interplanar distance (3.61 Å) than "a π-cloud thickness," and therefore have fairly poor overlap. However, two short S–S contacts are present between the **A** and **A**′ molecules, and the distances are 3.61 and 3.62 Å, which are shorter than a normal van der Waals' S–S contact (3.70 Å). The interplanar distance (3.47 Å) between **A**(**A**′) and **B** molecules is slightly shorter than "a π-cloud thickness," and the overlap is more effective than that between **A** and **A**′ molecules. Furthermore, there are significant contacts through the S atoms between the neighboring columns (Fig. 3b,c). The contact distance is 3.64 Å, a shorter van der Waals' S–S contact. Each $\mathrm{CuCl_4}$ anion is located near the **A**(**A**′) molecules so as to join the neighboring columns. The Cu–Cl bond distances are 2.23 and 2.29 Å, and the angles of each of two Cl–Cu–Cl bonds are 89.8, 111.8, 126.5 and 131.9°. From the above results, the geometry around the Cu atom in the $\mathrm{CuCl_4}$ anion is distorted-tetrahedral. The close contacts are present between two S (S(8) and S(24)) atoms in the 1,3-dithiole rings of **A**(**A**′) and **B** molecules, and one Cl (Cl(1)) atom of the $\mathrm{CuCl_4}$ anion (Fig. 5). The distances are 3.09 Å for the S(8)–Cl(1) contact and 3.30 Å for the S(24)–Cl(1) contact, which are considerably shorter than the sum (3.65 Å) of the van der Waals' radii of the S and Cl atoms.[19] On the other hand, contrary to our expectation, there is no close contact between the thiocarbonyl S atoms of **A**(**A**′) and **B** molecules, and the Cl atoms of the $\mathrm{CuCl_4}$ anion.

ESR spectra

For $(\mathbf{1})_2\cdot\mathrm{CuCl_4}$ the ESR spectrum at 298 K showed only two signals due to the Cu(II) spin at $g_{//}=2.0473$ and $g_{\perp}=2.2020$. When this result is considered together with the crystal structure, it is obvious that this $\mathrm{CuCl_4}$ salt can be actually represented as $(\mathbf{1}^{+\cdot})_2\cdot\mathrm{CuCl_4^{2-}}$ ($\mathbf{1}^{+\cdot}$: the radical cation of **1**) and the Cu(II) ($S=1/2$) spin only survives as a result of singlet dimer formation of $\mathbf{1}^{+\cdot}$ molecules.

On the other hand, the ESR spectra of the $(\mathbf{2})_3\cdot\mathrm{CuCl_4}$ microcrystals were measured at 298 and 77 K (Fig. 6). One doublet signal with very weak intensity was observed at $g=2.0052$ together with a strong broad signal due to the Cu(II) spins near $g=2.0932$ at 298 K. Since the lower *g* value is almost equal to those observed for several radical cation salts of **2** with non-magnetic counter-anions it can be reasonably assigned to the spin of conducting π electrons on the **2**-stacked column. The fact that the signals due to both spins of conducting π electrons and Cu(II) anions are separately observed at 298 K, suggests no π/d interaction at this temperature. On the other hand, in the spectrum at 77 K the signal at $g=2.0052$ disappeared. This fact suggests the possibility of significant interaction between conducting π electrons and Cu(II) d spins. Furthermore, the signals due to the d spins were observed separately at $g_{//}=2.0669$ and $g_{\perp}=2.2360$ and their intensity increased at 298 K.

Electrical resistivities

As expected from the tight dimerization of **1** molecules in $(\mathbf{1})_2\cdot\mathrm{CuCl_4}$, the ρ value on the single crystal was high ($3\times10^4\ \Omega\,\mathrm{cm}$) at 300 K. The single crystal of $(\mathbf{2})_3\cdot\mathrm{CuCl_4}$ showed a comparatively low ρ value ($0.6\ \Omega\,\mathrm{cm}$) at 300 K. The temperature dependence of ρ showed a semiconducting behavior in the temperature range 300 to 120 K, as seen in Fig. 7a. From the plot of ρ against T^{-1} the activation energy (E_a) in the higher temperature region was calculated to be 0.15 eV, but in the lower temperature region a gradual decrease

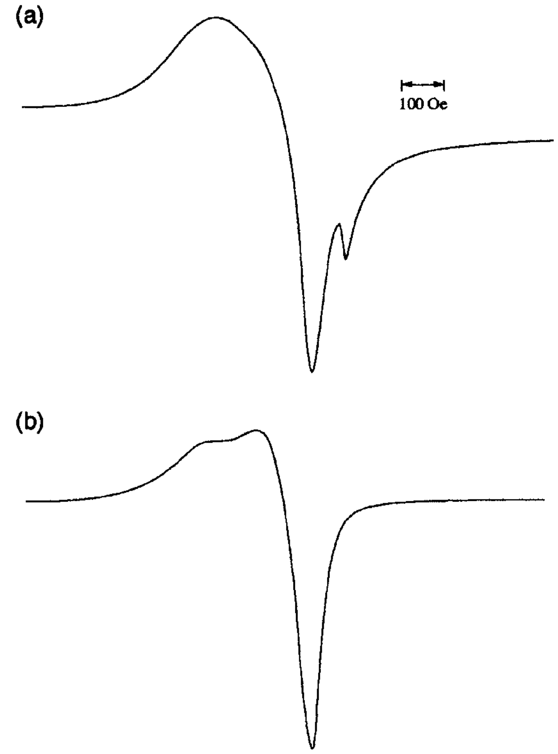

Fig. 6 Microcrystal ESR spectra of $(\mathbf{2})_3\cdot CuCl_4$ at (a) 298 and (b) 77 K.

in E_a was observed (see Fig. 7b). The pressure effect on ρ was also investigated. The ρ–T plots measured under atmospheric pressure, 4.9, 9.5 and 13.4 kbar are also shown in Fig. 7a. By increasing the pressure from atmospheric to 4.9 kbar, the ρ value decreased by 1/5. However, further increase of pressure from 4.9 to 9.5 and to 13.4 kbar only resulted in a small decrease in ρ. The ρ–T behavior was still semiconducting even at 13.4 kbar, although the E_a value gradually decreased from 0.13 eV (4.9 kbar) to 0.10 eV (9.5 kbar) and furthermore to 0.085 eV (13.4 kbar).

Magnetic susceptibilities

The temperature dependence of χ_p was investigated using microcrystalline samples of $(\mathbf{1})_2\cdot CuCl_4$ and $(\mathbf{2})_3\cdot CuCl_4$. Figs. 8 and 9 show the temperature dependences of the product of χ_p with T (χ_pT) in the temperature range 5 to 300 K for $(\mathbf{1})_2\cdot CuCl_4$ and $(\mathbf{2})_3\cdot CuCl_4$, respectively. For $(\mathbf{1})_2\cdot CuCl_4$ the χ_pT value was almost constant between 300 and 10 K, and below 10 K it decreased slightly with decreasing temperature. This can be interpreted as a χ_p–T behavior obeying a Curie–Weiss law [$\chi_p = C/(T-\theta)$ where C is the Curie constant and θ the Weiss temperature] with a very small θ value. Values which best reproduced the experimental results were $C =$ 0.379 emu K f.u.$^{-1}$ (f.u. $= (\mathbf{1})_2\cdot CuCl_4$) and $\theta = -0.1$ K.

On the other hand, for $(\mathbf{2})_3\cdot CuCl_4$ a gradual decrease in χ_pT was observed on cooling from 300 to *ca.* 170 K. Between *ca.* 170 and 20 K χ_pT was almost constant and below 20 K decreased again on cooling. The χ_p–T behavior in the temperature region 300 to *ca.* 170 K did not obey a Curie–Weiss law. Instead, when a temperature-independent χ_p (χ_π) was considered as another contributor, the observed χ_p–T behavior could be reasonably interpreted by an equation of the form $\chi_p = C/(T-\theta) + \chi_\pi$. The χ_π value is associated with the spins of the conducting π electrons on the **2**-stacked column. If the conduction is metallic, χ_p is of a Pauli-type. In the semiconducting case χ_π corresponds to an almost temperature-independent χ_p in the low-temperature region of the χ_p–T curve obtained by strongly antiferromagnetically-interacting spins. This $CuCl_4$ salt is a semiconductor, so that in this case χ_p has the latter physical meaning. The C, θ and χ_π values which best reproduced the experimental data were 0.388 emu K f.u.$^{-1}$ (f.u. $= (\mathbf{2})_3\cdot CuCl_4$), $+3.1$ K and 4.5×10^{-4} emu f.u.$^{-1}$, respectively. The obtained C is close to the value for one Cu(II) ($S =$ 1/2) spin entity, and the small and positive θ value shows weak ferromagnetic interaction. The χ_p is near the values [(2–11) $\times 10^{-4}$ emu f.u.$^{-1}$] obtained for several organic semiconductors reported so far.[3,20,21] On the other hand, below *ca.* 170 K the χ_p–T behavior obeyed a Curie–Weiss law, where C is 0.470 emu K f.u.$^{-1}$ and θ is -0.5 K. The zero point in χ_π suggests that the conducting π electrons actually disappear, instead, two π spins per three molecules of **2** are localized, forcing strong antiferromagnetic interactions which give rise to a marked decrease in their magnetic moments.

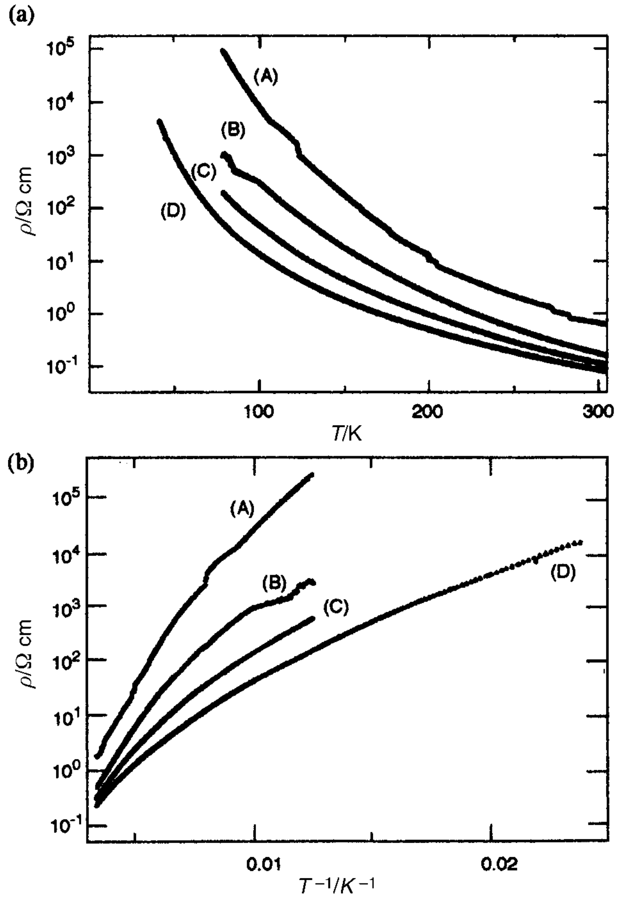

Fig. 7 Plots of ρ against (a) T and (b) T^{-1} on the single crystal of $(\mathbf{2})_3\cdot CuCl_4$ under (A) atmospheric pressure, (B) 4.9, (C) 9.5 and (D) 13.4 kbar.

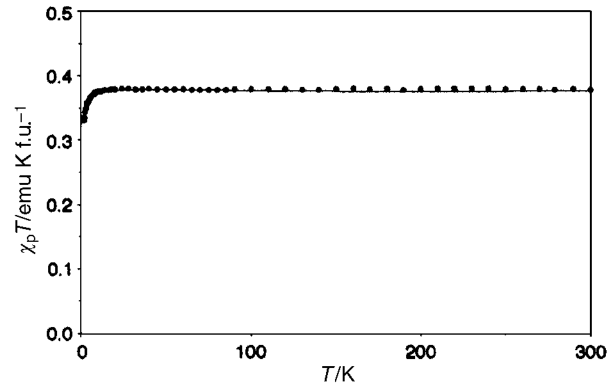

Fig. 8 Temperature dependence of χ_pT in the temperature range 5 to 300 K for microcrystals of $(\mathbf{1})_2\cdot CuCl_4$. The solid line is the fitting curve of $\chi_p = C/(T-\theta)$ ($C = 0.379$ emu K f.u.$^{-1}$ and $\theta = -0.1$ K).

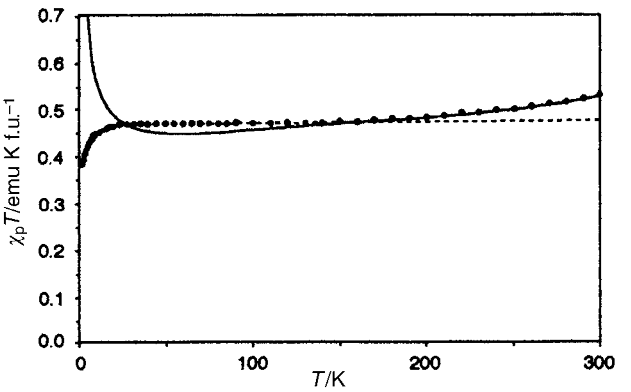

Fig. 9 Temperature dependence of $\chi_p T$ in the temperature range 5 to 300 K for microcrystals of $(\mathbf{2})_3\cdot CuCl_4$. The solid and dashed lines are the fitting curves of $\chi_p = C/(T-\theta)+\chi_\pi$ ($C = 0.388$ emu K f.u.$^{-1}$, $\theta = +3.1$ K and $\chi_\pi = 4.5\times10^{-4}$ emu f.u.$^{-1}$) between 300 and 150 K, and of $\chi_p = C/(T-\theta)$ ($C = 0.470$ emu K f.u.$^{-1}$ and $\theta = -0.5$ K) between 150 and 5 K, respectively.

Correlation of change in the χ_p–T behavior near 170 K with the crystal structure for $(\mathbf{2})_3\cdot CuCl_4$

In order to understand the origin of the change in the χ_p–T behavior near 170 K for $(\mathbf{2})_3\cdot CuCl_4$, the crystal structures at 293, 200 and 120 K were compared. Table 2 summarizes the interplanar distances (d) between least-squares planes in **A**/**A′** and **A**(**A′**)/**B** contacts. When this result is considered together with the cell constants and volumes shown in Table 1, a very large difference is recognized in the cell constant along the b axis, the **2**-stacked direction and also in the volume between 293 and 200 K. In particular, the d value in the **A**/**A′** contact with very small overlap becomes shorter by 0.04 Å while the changes noted above become considerably smaller between 200 and 120 K. From these results more effective overlap in the **2**-stacked column is indeed achieved on cooling. This represents increased suppression of semiconducting behavior, and indeed a gradual decrease in E_a was observed in the lower temperature region. The short contact between **A**(**A′**) or the **B** molecule and the $CuCl_4$ anion was compared between 293, 200 and 120 K. The results are shown in Table 3. The short contacts are present between the S atoms on the 1,3-dithiole ring of the **A**(**A′**) or **B** molecules and one Cl atom on the $CuCl_4$ anion, *i.e.*, S(8)···Cl(1) and S(9)···Cl(1) in the **A**(**A′**)/$CuCl_4$ contact and S(24)···Cl(1) in the **B**/$CuCl_4$ contact. Their distances are 3.44, 3.39 and 3.43 Å at 293 K, 3.09, 3.67 and 3.30 Å at 200 K, and 3.08, 3.67 and 3.29 Å at 120 K, respectively. The three short distances markedly increase or decrease on cooling from 293 to 200 K, but show almost no change between 200 and 120 K. The S(8)···Cl(1) distances at 200 and 120 K are 3.09 and 3.08 Å, respectively, which are remarkably shorter than the sum (3.65 Å) of the van der Waals' radii of the S and Cl atoms. In addition, the MOPAC MO calculations show that some electron densities in the highest-occupied MO of **2** are present on the 1,3-dithiole ring (0.0239 and 0.0345) and thiocarbonyl S atoms (0.0009). Accordingly, these results suggest significant interaction between conducting π electrons on the **2**-stacked column and localized Cu(II) d spins on the $CuCl_4$ anions, rather than a mere transformation of the **2**-stacked column structure, as the most plausible reason for the change in the χ_p–T behavior near 170 K.

Table 2 Intermolecular distances (d/Å) between least-squares plane contacts in **A**/**A′** and **A**(**A′**)/**B** at 293, 200 and 120 K

	d	
T/K	**A**/**A′**	**A**(**A′**)/**B**
293	3.65	3.44
200	3.61	3.47
120	3.59	3.45

Table 3 Short distances (Å) between the S atom on the 1,3-dithiole ring of **A**/**A′** or **B** molecule and one Cl atom on the $CuCl_4$ ion at 293, 200 and 120 K

T/K	**A**(**A′**)/$CuCl_4$ (S(8)···Cl(1))	**A**(**A′**)/$CuCl_4$ (S(9)···Cl(1))	**B**/$CuCl_4$ (S(24)···Cl(1))
293	3.44	3.39	3.43
200	3.09	3.67	3.30
120	3.08	3.67	3.29

Conclusions

The two $CuCl_4$ salts of new donor molecules **1** and **2** were synthesized. For $(\mathbf{1})_2\cdot CuCl_4$ a high ρ value was observed at room temperature. Furthermore, the Cu(II) spins in the $CuCl_4$ anions only survive as a result of the dimerization of **1** molecules. On the other hand, $(\mathbf{2})_3\cdot CuCl_4$ exhibited a relatively low ρ value at room temperature, but the temperature dependence of ρ was semiconducting. CuX_4 (X = Cl, Br) salts with a similar molecular formula to those of $(\mathbf{2})_3\cdot CuCl_4$, (BEDT-TTF)$_3\cdot CuCl_4\cdot H_2O$,[5] (BEDT-TTF)$_3\cdot CuBr_4$[10] and (BEDT-TTF)$_3\cdot CuCl_2Br_2$[10] are already known in which both low ρ values at room temperature, and metallic or semiconducting behavior are observed. Furthermore, for these CuX_4 salts it was demonstrated that significant interaction indeed occurs between conducting π electrons on the BEDT-TTF-stacked column and local Cu(II) d spins on the CuX_4 anions albeit at very low temperatures. In contrast to these, it is most probable that $(\mathbf{2})_3\cdot CuCl_4$ exhibits significant interaction between conducting π electrons on the **2**-stacked column and localized Cu(II) d spins on the $CuCl_4$ anions even at the relatively high temperature of *ca.* 170 K. It is conceivable that the close contact occurs between the S atoms on the 1,3-dithiole ring projected from the dihydrotetrathiafulvalene skeleton and one Cl atom on the $CuCl_4$ anion near this temperature. However, much more definitive conclusions on the nature and mechanism of this π/d interaction must be obtained by further investigation.

Acknowledgements

This work was supported by a Grant-in-Aid for Scientific Research on Priority Areas (B) (No. 11224209) from the Ministry of Education, Science and Culture, Japan.

References

1 P. Day, *Philos. Trans. R. Soc. London, Ser. A*, 1985, **314**, 145.
2 C. J. Schramm, R. P. Scaringe, D. R. Stojacobic, B. M. Hoffman, J. A. Ibers and T. J. Marks, *J. Am. Chem. Soc.*, 1980, **102**, 6702.
3 H. Yamakado, T. Ida, A. Ugawa, K. Yakushi, K. Awaga, Y. Maruyama, K. Imaeda and H. Inokuchi, *Synth. Met.*, 1994, **62**, 169.
4 A. Aumüller, P. Erk, G. Klebe, S. Hünig, J. U. von Schütz and H.-P. Werner, *Angew. Chem.*, 1986, **98**, 759; A. Aumüller, P. Erk, G. Klebe, S. Hünig, J. U. von Schütz and H.-P. Werner, *Angew. Chem., Int. Ed. Engl.*, 1986, **25**, 740.
5 P. Day, M. Kurmoo, T. Mallah, I. R. Marsden, M. L. Allan, R. H. Friend, F. L. Pratt, W. Hayes, D. Chasseau, J. Gaultier, G. Bravic and L. Ducasse, *J. Am. Chem. Soc.*, 1992, **114**, 10722.
6 T. Enoki, J. Yamaura, N. Sugiyasu, K. Suzuki and G. Saito, *Mol. Cryst. Liq. Cryst. Sci. Technol., Sect. A*, 1993, **233**, 325.
7 J. Martinsen, J. L. Stanton, R. L. Greene, J. Tanaka, B. M. Hoffman and J. A. Ibers, *J. Am. Chem. Soc.*, 1985, **107**, 6915.
8 A. Kobayashi, T. Udagawa, H. Tomita, T. Naito and H. Kobayashi, *Chem. Lett.*, 1993, 2179.

9 A. Aumüller and S. Hünig, *Liebigs Ann. Chem.*, 1989, 142.

10 I. R. Marsden, M. L. Allan, R. H. Friend, M. Kurmoo, D. Kanazawa, P. Day, G. Bravic, D. Chasseau, L. Ducasse and W. Hayes, *Phys. Rev. B: Solid State*, 1994, **50**, 2118.

11 H. Kobayashi, H. Tomita, T. Naito, A. Kobayashi, F. Sakai, T. Watanabe and P. Cassoux, *J. Am. Chem. Soc.*, 1996, **118**, 368.

12 E. Ojima, H. Fujiwara, K. Kato, H. Kobayashi, H. Tanaka, A. Kobayashi, M. Tokumoto and P. Cassoux, *J. Am. Chem. Soc.*, 1999, **121**, 5581.

13 M. Iwamatsu, T. Kominami, K. Ueda, T. Sugimoto, H. Fujita and T. Adachi, *Chem. Lett.*, 1999, 329; M. Iwamatsu, T. Kominami, K. Ueda, T. Sugimoto, T. Adachi, H. Fujita, H. Yoshino, Y. Mizuno, K. Murata and M. Shiro, *Inorg. Chem.*, 2000, **39**, 3810.

14 K. Ueda, M. Yamanoha, T. Sugimoto, H. Fujita, A. Ugawa, K. Yakushi and K. Kano, *Chem. Lett.*, 1997, 461.

15 E. Klingsberg, *J. Am. Chem. Soc.*, 1964, **86**, 5290.

16 F. Wudl and M. L. Kaplan, *J. Org. Chem.*, 1974, **24**, 3608.

17 *teXsan*, Crystal Structure Analysis Package, Molecular Structure Corporation, Houston, TX, 1985 and 1992.

18 G. A. Jeffrey and R. Shiono, *Acta Crystallogr.*, 1959, **12**, 447.

19 L. Pauling, *The Nature of the Chemical Bond*, 3rd edn., Cornell University Press, Ithaca, New York, 1960.

20 K. Ueda, M. Goto, M. Iwamatsu, T. Sugimoto, S. Endo, N. Toyota, K. Yamamoto and H. Fujita, *J. Mater. Chem.*, 1998, **8**, 2195.

21 K. Ueda, Y. Kamata, M. Iwamatsu, T. Sugimoto and H. Fujita, *J. Mater. Chem.*, 1999, **9**, 2979.